

# Glove-Integrated Slotted Patch Antenna for Wearable UHF RFID Reader

Shahbaz Ahmed  
Faculty of Biomedical Sciences and  
Engineering  
Tampere University of Technology  
Tampere, Finland  
shahbaz.ahmed@tut.fi

S. M. Musfequr Rehman  
Faculty of Electronics and  
Communications Engineering  
Tampere University of Technology  
Tampere, Finland  
s.rahman@student.tut.fi

Leena Ukkonen  
Faculty of Biomedical Sciences and  
Engineering  
Tampere University of Technology  
Tampere, Finland  
leena.ukkonen@tut.fi

Toni Björninen  
Faculty of Biomedical Sciences and  
Engineering  
Tampere University of Technology  
Tampere, Finland  
toni.bjorninen@tut.fi

**Abstract**—We present a glove-integrated slotted patch antenna for a wearable Ultra High Frequency Radio Identification Technology (UHF RFID) reader operating at 866 MHz. We tested the prototype antenna made of copper foil adhered on low-permittivity Ethylene Propylene Diene Monomer (EPDM) foam material having the thickness of 4 mm. To characterize the antenna, we tested it wirelessly in communication with a common dipole type RFID tag to estimate its realized gain, radiation pattern and maximum tag read range it provides. We also analyzed the effects of variable separation between the antenna and the body to confirm stable operation required by the application. The results showed that the antenna feasible for the work glove applications providing the read range up to 360 cm with the reader's output power of 28.4 dBm.

**Keywords**— *slotted patch antenna; RFID reader antenna; UHF; wearable antenna; work glove application.*

## I. INTRODUCTION

Radio Frequency Identification Technology (RFID) has widely been deployed for short distance communication within Ultra High Frequency (UHF) band, with industrial applications in the areas of supply chain management to biomedical applications [1]. In such systems, the antennas act as the backbone of communication. The efficiency and reliability of wireless communication links between the wearable devices and the surrounding, directly depends on the antennas. Particularly, the wearable antennas play a significant role in the communication between the wireless communication link between the Body Area Networks (BANs). The wearable antennas should be flexible, comfortable, lightweight, cost effective and maintenance free. A typical RFID system operates in the frequency range of 860-960 MHz frequency band [2]. With the advancement in the electro-textiles and conductive wearable materials, there is a lot more work done on the wearable tag antennas, than the wearable reader antennas for the BAN. However, some of the body worn RFID reader antennas have been developed with nonflexible materials as substrate and radiating element. [3] presents a wearable RFID reader antenna, fabricated with copper foil and FR-4 as a substrate. In [4], a RFID reader was placed on the glove, with a maximum read range of 7.6 cm. Another RFID reader antenna fabricated on nonflexible FR-4 epoxy substrate and tuned at resonance frequency of 2.4 GHz is presented in [5].

In general, the recent studies have focused on the fabrication of the wearable RFID reader antennas using nonflexible substrates [3-5]. In this paper, we have simulated and fabricated a slotted patch reader antenna for UHF RFID system, on flexible Ethylene Propylene Diene Monomer (EPDM) material. We also focused on increasing the read range of the antenna in accordance with the application requirement. Using EPDM material as substrate leverages the wearability and integrability of the antenna to the work glove with promising read range for the RFID system.

This paper is structured as follows. Section II, describes the geometry and results obtained for the tag which is used in the measurement of RFID reader antenna results. In section III, authors describe the planar human hand model for simulating and optimizing the RFID reader antenna in ANSYS HFSS v16. The section III also presents the electromagnetic properties of different layers of human tissues. In section IV, the antenna development and simulation results are discussed i.e. the simulated reflection coefficient, the 3D radiation pattern and the surface current density. This section presents the geometry of the antenna. Section V focuses on the measured results from different demonstrations. Section VI concludes the paper and presents the future work.

## II. TAG DEVELOPMENT

In the electromagnetic modelling, we used ANSYS High Frequency Structure Simulator (HFSS). To model the RFID IC, we used an equivalent parallel connection of resistance and capacitance of 2.85 k $\Omega$  and 0.91 pF, respectively [7]. From the modelling, we obtained the antenna impedance, the radiation efficiency and computed the realized gain of the tag at 866 MHz frequency. Using this data, we were able to predict the read range and the realized gain of the tag. Fig. 1 shows the geometry of the tag antenna, whereas, table. 1 shows the tag dimensions. We measured the threshold power  $P_{th,min}$ , that is the minimum power required to activate the tag. We used the RFID IC wake up power  $P_{ic0}$  and the path loss  $L_{iso}$  in the wireless measurement channel, defined by the output port of transmitter to the input port of a hypothetical isotropic antenna separated by a distance, to calculate the realized gain of the tag antenna as [10]

$$G_{r(tag)} = \frac{P_{ic0}}{L_{iso} P_{th,min}}. \quad (1)$$

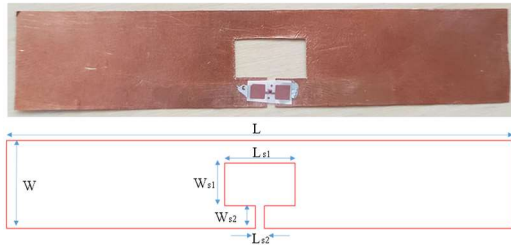


Fig. 1. Dimensions and prototype of the slotted patch antenna.

TABLE 1. DIMENSION OF DIPOLE TAG ANTENNA

Geometrical Parameter	Value
Length (L)	113 mm
Width (W)	20 mm
Length of slot 1 ( $L_{s1}$ )	15.7 mm
Width of slot 1 ( $W_{s1}$ )	9.7 mm
Length of slot 2 ( $L_{s2}$ )	5.15 mm
Width of slot 2 ( $W_{s2}$ )	2 mm

As seen in the Fig. 2, the realized gain of the antenna is almost -0.17 dBi at 866 MHz frequency. It can be seen that tag shows promising read range over the bandwidth of 863-872 MHz, which is the band of the RFID reader antenna for the glove application.

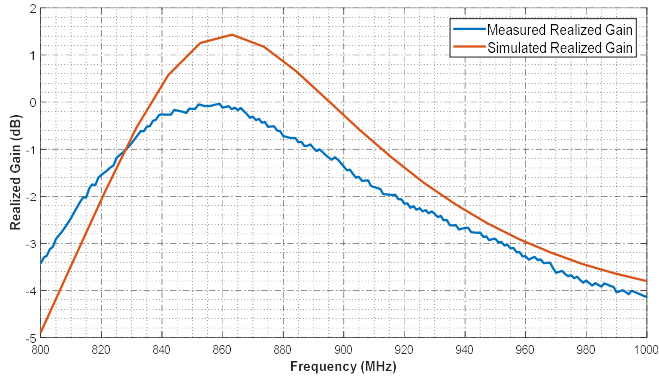


Fig. 2. Measured and simulated realized gain of the dipole tag.

### III. HUMAN HAND MODEL

The human hand model used for the simulation was composed of seven layers—skin, fat, muscle, bone cortical, muscle, fat and bone. From the electromagnetic point of view, all the layers are lossy dielectrics with specific thickness and complex permittivities [7].

In the simulation model, the skin, fat, muscle, and cortical bone are planar layers with frequency dependent electromagnetic properties i.e. the permittivity, the loss tangent, and the conductivity shown in Fig. 4. The configuration and dimensions of the multilayer models for the hand are shown in Fig. 3 and table. 2 respectively. The hand model is a block of dimension 11 cm  $\times$  30 cm, whereas, the height of the block is given by the thickness of the individual layers. The electrical properties of these layers can vary from person to person. The fat is a reservoir of energy and heat insulator. It is impossible to determine the thickness of the fat layer as they depend on the individual human anatomy. Similarly, the muscles are elastic in nature, having the ability to relax and contract, which in turn defines the thickness of the muscle. However, the nominal thicknesses are selected for the implementation of the planar human hand model and are shown in Fig. 3.

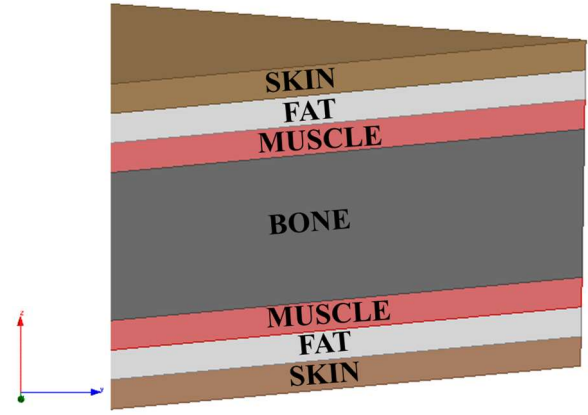


Fig. 3. Planar human hand model for simulations.

TABLE 2. DIMENSIONS OF PLANAR HUMAN HAND MODEL.

Tissue layer	Thickness (mm)
Skin	2 mm
Fat	2 mm
Muscle	2 mm
Bone	10 mm
Muscle	2 mm
Fat	2 mm
Skin	2 mm

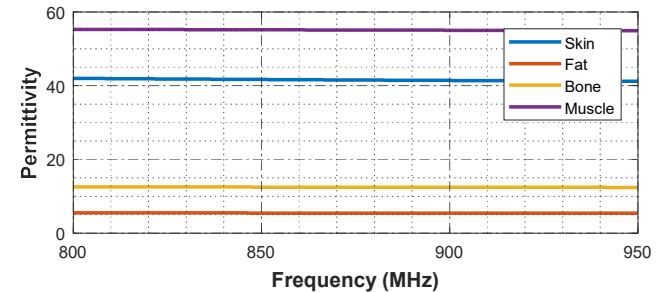
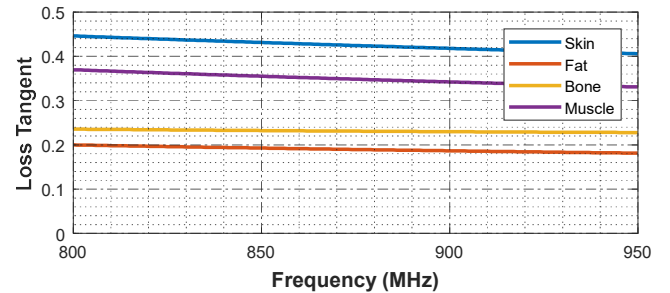
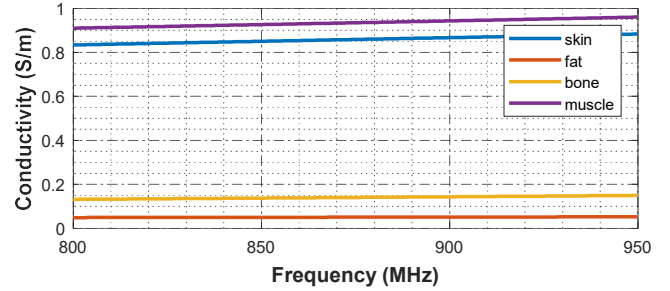


Fig. 4. Conductivity of skin, fat, bone, and muscle (Top), Loss tangent of skin, fat, bone, and muscle (middle), Permittivity of skin, fat, bone, and muscle (bottom).

#### IV. USING THE TEMPLATE

The fundamental challenge in the development of the reader antenna is the miniaturization for exact form factor suitable for our work glove application. The first challenge is the development of an antenna with less influence of human body's electrical properties and higher gain in the proximity of the human body. For this reason, the patch antenna seems to be a good candidate because it possesses a ground plane, which acts as an insulator between the patch of the antenna and the human body. Another challenge is to attain the exact form factor through miniaturization, without compromising the efficiency and the gain of the antenna. In literature, researchers have discussed various miniaturization techniques i.e. using high permittivity materials as substrate, meandering of the patch by inserting the spiraling, inserting slots [8] and lines to elongate the length of the current path, grounding of the patch through a pin [9], using metamaterials [10-12] and inverted F configuration. Despite of miniaturized structures and promising electromagnetic performances, these above-mentioned structures are rigid with significant thickness, which makes them not befitting our application, as form factor along with flexibility is our priority.

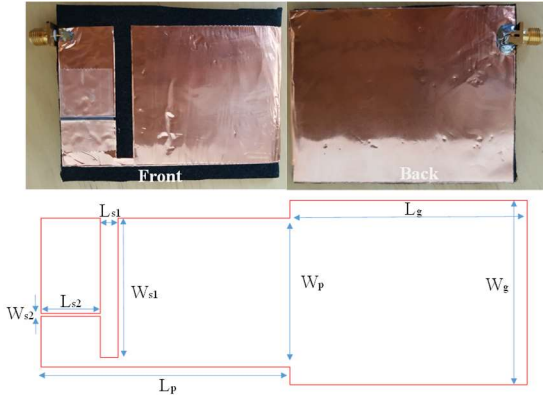


Fig. 5. Fabricated slotted patch antenna (top). Dimension of the slotted patch antennas (bottom).

Fig. 5 shows the fabricated slotted patch antenna with dimensions. ANSYS HFSS v.16 is used for the antenna optimization. The planar human hand model shown in Fig. 3 with the electromagnetic properties presented in Fig. 4, is used to tune the antenna at a resonance frequency of 866 MHz. The antenna dimensions are used to resonate around 863-872 MHz, which covers the targeted RFID frequency band. Two slots are introduced to miniaturize the antenna and to tune the antenna at 866 MHz.

TABLE 3. DIMENSIONS OF THE SLOTTED PATCH ANTENNA

Geometric Parameters	Value
Length of patch ( $L_p$ )	84 mm
Width of patch ( $W_p$ )	50 mm
Length of ground ( $L_g$ )	80 mm
Width of ground ( $W_g$ )	62 mm
Length of slot 1 ( $L_{s1}$ )	6 mm
Width of slot 1 ( $W_{s1}$ )	46.8 mm
Length of slot 2 ( $L_{s2}$ )	20 mm
Width of slot 2 ( $W_{s2}$ )	1 mm
Substrate thickness ( $h$ )	4 mm

The antenna is fabricated on EPDM foam material (commonly used in wearables) as substrate with the dimensions of 60mm  $\times$  80mm  $\times$  4mm, dielectric constant ( $\epsilon_r$ )

1.26 and the loss tangent ( $\delta$ ) 0.007. An adhesive copper tape having thickness of 35  $\mu$ m is used to fabricate the ground and the patch of the antenna as shown in Fig. 5.

Fig. 6 shows the simulation results of the antenna reflection coefficient, when mounted on the hand glove. However, the shift in the resonance frequency is observed from the reflection coefficient, due to the inaccuracies in the fabrication of the antenna on the flexible substrate, as the flexibility causes transformation of the antenna geometry. The -10 dB bandwidth of the antenna is 13 MHz (from 863 MHz to 872 MHz) and at 866 MHz the antenna reflection coefficient is -11 dB. In the simulation, we have observed that the width  $W_{s1}$  has significant effect on the fine-tuning of the resonance frequency.

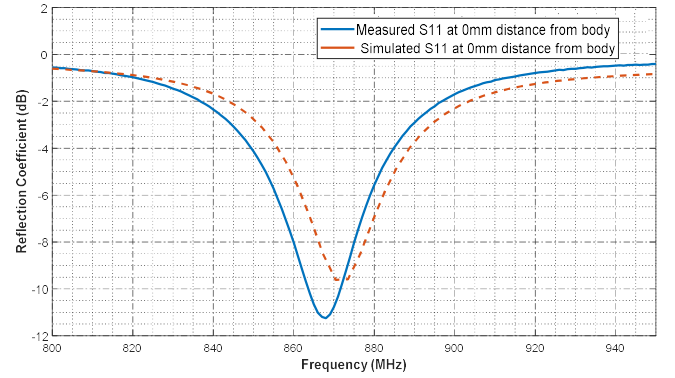


Fig. 6. Measured and simulated reflection coefficient on body.

The near body simulation showed the peak gain of the antenna is -0.14 dBi. The peak gain of the antenna is decreased due to the miniaturization technique applied to fit the antenna on human hand. The 3D radiation pattern is shown in Fig. 7. The main aim of the pattern shaping is to maintain the maximum gain in the +z and +y direction, away from the body, to attain maximum read range. As seen from the Fig. 7, the radiation intensity is maximum in +z and +y direction.

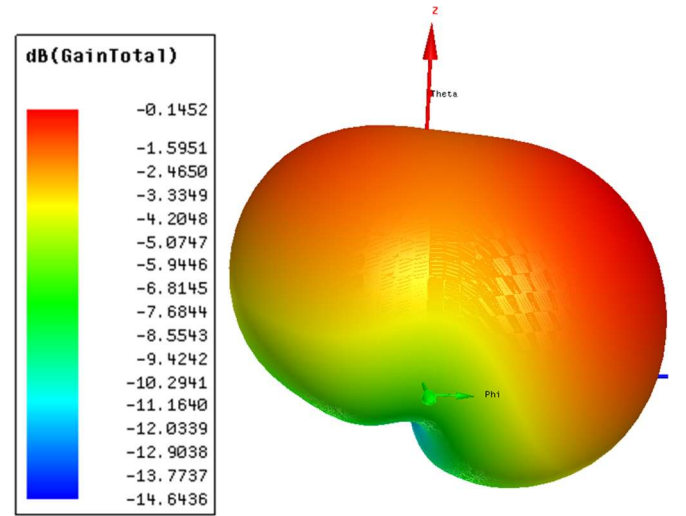


Fig. 7. 3D Radiation pattern of the UHF RFID reader slotted patch antenna.

Fig. 8 presents the surface current distribution of the antenna. It is evident that the width of the slot  $W_{s1}$  plays a

significant role in the fine-tuning of the antenna at 866 MHz frequency and the edges have the higher current surface density and hence are more radiative edges.

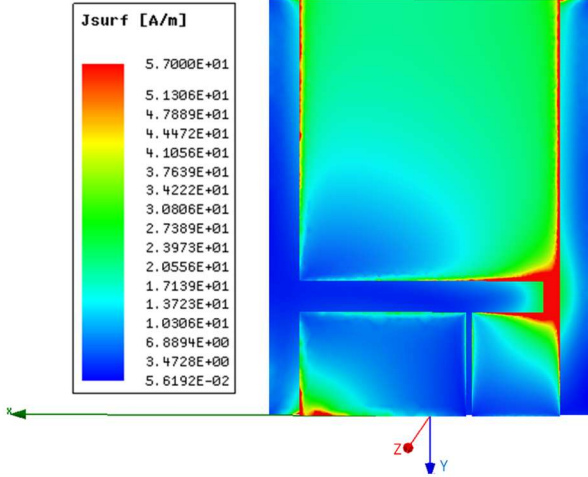


Fig. 8 Complex magnitude of surface current distribution on the patch surface.

The simulated antenna directivity is 2.37 dB whereas the radiation efficiency is 40.7% at 866 MHz.

## V. MEASUREMENT AND RESULTS

After the optimization procedure through simulation, the antenna was fabricated on a flexible EPDM substrate. The antenna was mounted on hand. We performed three different measurements. In the first measurement, we measured the reflection coefficient of the antenna at different distances from the human hand to analyze the impact of the varying distance between the antenna and the human hand. In the second measurement, we measured the threshold power and computed the realized gain calculations over the -10dB bandwidth of the antenna. In the third measurement, we measured the maximum read range by varying the transmitted power from the antenna.

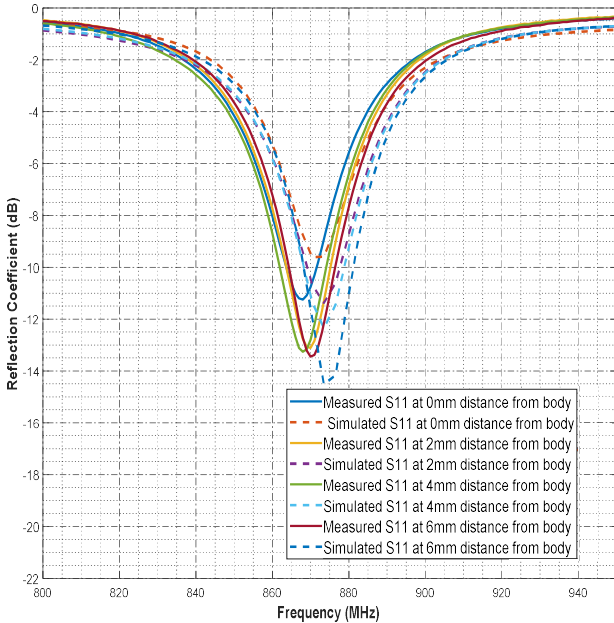


Fig. 9. Reflection coefficient of the antenna at different distances from the human hand.

In the first measurement, the antenna was attached to the Vector Network Analyzer (VNA) and the antenna was mounted on the human hand. Fig. 9 presents the reflection coefficient of the antenna at different distances from the human hand i.e. 0 mm, 2 mm, 4 mm and 6 mm. We observed some frequency shift to lower resonance frequencies in the measured and simulated reflection coefficients due to the inaccuracies in the fabrication of the antenna. It is evident that increasing the distance between the hand and the patch antenna improves the matching and increases the bandwidth of the antenna. Antenna bandwidth increased from 863-872 MHz to 860-877 MHz, which depicts that the antenna is stable to the varying air gaps between the antenna and hand human. The measurement of the reflection coefficient verifies the planar human hand model used for the simulation because the measured results has shown good agreement with the simulated results.

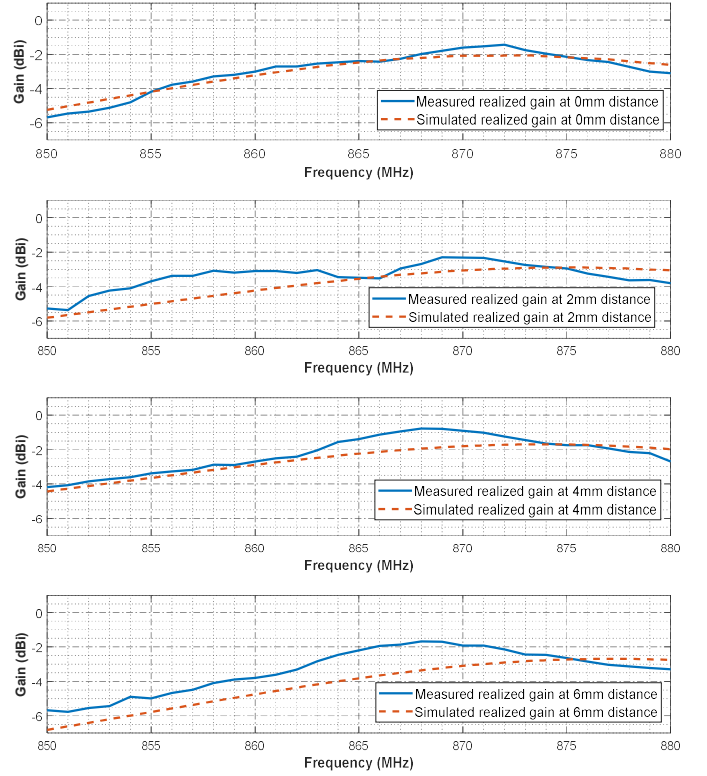


Fig. 10. Antenna realized gain on human hand (top), antenna realized gain at 2 mm separation between hand and antenna (second from top), antenna realized gain at 4 mm separation between hand and antenna (second from bottom), antenna realized gain at 6 mm separation from the body (bottom).

In the second measurement, the antenna mounted on the human hand, was attached to the Voyantic Tagformance equipment. The copper dipole tag—presented in the section II—was placed at a distance of 0.8 meters from the antenna and we measured the threshold power over the frequency range of 850-880 MHz. The realized antenna gain was estimated by the Friis transmission equation, given as [2]

$$G_R = \frac{P_{ic}}{G_{r,tag} L_{cab} \left(\frac{\lambda}{4\pi s}\right)^2 P_{th}}, \quad (2)$$

where  $P_{ic0}$  is the RFID IC wake up power equivalent to -18 dBm and provided by the manufacturer,  $L_{cab}$  is the cables losses of the Tagformance cable and is measured by using the two port configuration of the Vector Network Analyzer (VNA) and terminating the receiver port of the tagformance



with  $50 \Omega$  resistance. The value of  $L_{cab}$  was measured as  $-1.69$  dB, and  $P_{th}$  is the threshold power, which is the minimum power required to get the response from the tag and  $s$  is the separation between the antenna and the dipole tag. Whereas  $\lambda$  is defined by the transmission frequency of the antenna. In equation 2, the polarization mismatch is ignored, as it is negligible in our case. Fig. 10 shows the measured realized gain of the antenna at different distance between the human and the body. The simulated realized gain of the reader antenna can be obtained using

$$G_{R,realized} = G_R \times (1 - |\Gamma|^2), \quad (3)$$

where the measured realized gain of the antenna is  $-3$  dB, which is  $0.21$  dB more than that of the simulated realized gain. At  $0$  mm distance from the body, the measured realized gain shows good agreement with the simulation results over the frequency range of  $30$  MHz i.e.  $850$ - $880$  MHz. However, if the separation between the human hand and the antenna is increased, the difference between simulated and measured realized gain increases. Probable reason for this difference is the limitation of the planar human hand model, that it cannot map the solution for the gain estimation of the antenna and hence needs further modifications. However, the measurement results for the gain shows that the antenna is stable over the measured frequency range i.e. it maintains the performance even if the separation between the human and the antenna is variable.

In the third measurement, the antenna is radiated with varying transmission power at  $866$  MHz. The experiment was carried out in outdoor environment to minimize the effect of multi path propagation. The theoretical read range of the antenna being polarization match with the tag is attained and calculated from the simulated data as follow [2]

$$R_{ant} = \frac{\lambda}{4\pi} \sqrt{\frac{G_{ant}G_{r,tag}L_{cab}P_{tx}}{P_{ic}}}, \quad (4)$$

where  $G_{ant}$  and  $G_{r,tag}$  are the gains of the antenna and the tag respectively.  $L_{cab}$  is the cable losses and  $P_{tx}$  is the power transmitted by the antenna.

The results showed a good agreement between the theoretical read range and the measured read range of the antenna as shown in Fig. 11. The Voyantic Tagformance was able to transmit maximum power of  $28.4$  dBm at which we attained the read range of  $360$  cm. However, according to the theoretical read range computed by the Friis formula, if we transmit  $30$  dBm power,  $405.9$  cm of read range can be attained.

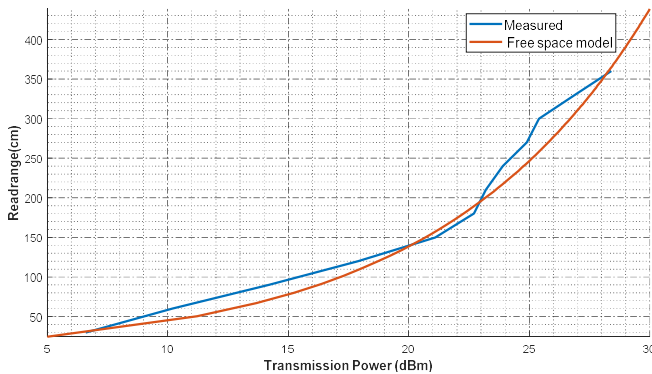


Fig. 11. Maximum read range with varying transmission powers at  $866$  MHz frequency.

## VI. CONCLUSION

We presented a wearable UHF RFID slotted patch reader antenna, developed from flexible EPDM material as substrate and copper tape as conductive part of the antenna. The antenna resonated at a frequency of  $866$  MHz. The comprehensive measurements have demonstrated that the antenna showed promising results for work glove application. At  $866$  MHz frequency, the antenna has  $-2.21$  dB gain and the maximum read range of  $360$  cm with the transmission power of  $28.4$  dBm. In addition to that, the demonstration verified that the antenna is stable to varying air gaps between the human hand and antenna. The simulation also depicts that the planar hand model used for tuning the antenna at  $866$  MHz is appropriate for the reflection coefficient, but needs modification for more accurate estimation of the antenna radiation properties.

## REFERENCES

- [1] K. Finkenzeller, RFID Handbook, 2nd ed., New York: Wiley, 2003, pp. 6-9.
- [2] K. Koski, L. Sydänheimo, Y. Rahmat-Samii and L. Ukkonen, "Fundamental characteristics of electro-textiles in wearable UHF RFID patch antennas for body-centric sensing systems," in IEEE Transactions on Antennas and Propagation, vol. 62, no. 12, pp. 6454-6462, Dec. 2014.
- [3] T. Campi et al., "A numerical dosimetry study of a wearable RFID reader antenna for navy personnel localization," IEEE International Symposium on Electromagnetic Compatibility (EMC), 16-22 Oct. 2015, Dresden, Germany, pp. 194-197.
- [4] L. Muguira et al., "RFIDGlove: A wearable RFID reader," IEEE International Conference on e-Business Engineering, 21-23 Oct. 2009, Macau, China, pp. 475-480.
- [5] I. Locher, M. Klemm, T. Kirstein and G. Trster, "Design and characterization of purely textile patch antennas," IEEE Transactions on Advanced Packaging, vol. 29, no. 4, pp. 777-788, Nov. 2006.
- [6] T. Björninen, L. Sydänheimo, and L. Ukkonen, "Development and validation of an equivalent circuit model for UHF RFID IC based on wireless tag measurements," Antenna Measurement Techniques Association Symposium, 21-26 Oct 2012, Bellevue, WA, USA, 6 pages.
- [7] H. Vladimír, "Planar antenna in proximity of human body models," 2013 7th European Conference on Antennas and Propagation (EuCAP), 8-12 Apr. 2013, Gothenburg, pp. 3309-3311.
- [8] S. I. Hussain Shah, S. Bashir and A. Altaf, "Miniaturization of microstrip patch antenna by using various shaped slots for wireless communication systems," International Seminar/Workshop on Direct and Inverse Problems of Electromagnetic and Acoustic Wave Theory (DIPED), 22-25 Sept. 2014, Tbilisi, pp. 92-95.
- [9] K. J. Anjali and C. D. Suriyakala, "A highly miniaturized patch antenna," International Conference on Circuit, Power and Computing Technologies (ICCPCT), 2017, Kollam, pp. 1-6.
- [10] M. Mehrparvar and F. H. Kashani, "Microstrip antenna miniaturization using metamaterial structures," Iranian Conference on Electrical Engineering (ICEE2012), 15-17 May. 2012, Tehran, pp. 1243-1246.
- [11] H. Yuan, S. Qu, J. Zhang, J. Wang and W. Li, "A novel miniaturized microstrip patch antenna based on metamaterial unit," IEEE 16th International Conference on Communication Technology (ICCT), 18-20 Oct. 2015, Hangzhou, pp. 606-607.
- [12] R. O. Ouedraogo and E. J. Rothwell, "Metamaterial inspired patch antenna miniaturization technique," IEEE Antennas and Propagation Society International Symposium, 11-17 Jul. 2010, Toronto, ON, pp. 1-4.